analytical chemistry

pubs.acs.org/ac Letter

Identification of Cell Status via Simultaneous Multitarget Imaging Using Programmable Scanning Electrochemical Microscopy

Xin Ning, Tao Wu, Qiang Xiong, Fan Zhang,* and Pin-Gang He*

Cite This: *Anal. Chem.* 2020, 92, 12111−12115 Read Online

ACCESS | Metrics & More | Article Recommendations | Supporting Information

ABSTRACT: A programmable multitarget-response electrochemical imaging technique was presented using scanning electrochemical microscopy (SECM) combined with a self-designed waveform. The potential waveform applied to the tip decreased the charging current caused by the potential switch, enhancing the signal-to-noise ratio. This programmable SECM (P-SECM) method was used to scan a metal strip for verifying its feasibility in feedback mode. Since it could achieve simultaneous multitarget imaging during one single imaging process, PC12 cells status was imaged and identified through three different molecules (FcMeOH, $Ru(NH_3)_6^{3+}$, and oxygen). The FcMeOH image eliminated the error from cell height, and the $Ru(NH_3)_6^{3+}$ image verified the change of membrane permeability. Moreover, the oxygen image demonstrated the bioactivity of the cell via its intensity of respiration. Combining information from these three molecules, the cell status could be determined accurately and also the error caused by time consumption with multiple scans in traditional SECM was eliminated.

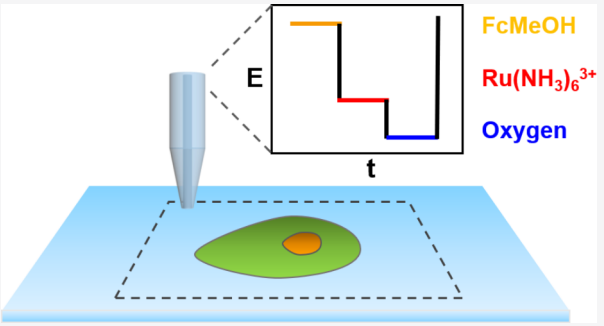

Cell imaging techniques occupy an important position in the identification of cell's vital activity. The optical imaging methods have been used for cell imaging in many aspects,[1] like measuring properties of molecular and cellular movements,[2,3] the cellular location of biomolecules,[4] and interactions between biomolecules.[5] Compared with the optical method, the electrochemical imaging method exhibited better sensitivity. However, most electrochemical imaging was the reflection of one mediator,[6] which means that the imaging information was relatively single and it might not be possible to observe the correlation between different molecules in a given state of cells.

Scanning electrochemical microscopy (SECM)[7] is an advanced technology for electrochemical imaging of cells with high sensitivity and no fixing of cells[6,8,9] but few limitations. One is that only a single molecule can be measured in one single imaging,[10] and renewed scans need to be started if more information from different molecules is required. Thus, it is impossible to simultaneously obtain the imaging information, corresponding to kinds of molecules. A quad-probe multifunctional tip invented by Unwin's group[11] permitted the simultaneous detection of multiple targets. However, its procedure of making a tip responsive to more-than-two targets might be complicated. It had been reported that fast-scan cyclic voltammetry SECM made the simultaneous detection of different molecules,[12] but its high charging current decreased the signal-to-noise ratio. Potential pulse-based SECM developed by Schumann's group exhibited a multitarget response in the oxygen reduction reaction,[13] but it also lacks the means to decrease the charging current caused by the long-range potential switch, which might lead to inaccuracy and distortion of cell imaging. Therefore, it will be significant if several molecules, which are relative to cell status or vital activities, can be imaged in a single imaging with a simple ultramicroelectrode and low charging current. Thus, more accurate information would be obtained and used for analyzing the relationship between relative molecules at a particular cell status.

Herein, we developed a new programmable SECM (P-SECM) technology for obtaining a multitarget response in one single image. A self-designed waveform for multitarget response was executed, instead of constant potential, at each scanning site (Figure 1). This new P-SECM method was first applied to scan a metal strip for verifying its feasibility in feedback mode. The waveform and data analysis decreased the charging current, enhancing the signal-to-noise ratio. Three different redox mediators would be used for cell imaging by P-SECM. Also, the comparison of cells at different statuses imaged by these mediators in the same imaging period would also be discussed. This technique provided accurate

Received: June 9, 2020
Accepted: August 17, 2020
Published: August 17, 2020

https://dx.doi.org/10.1021/acs.analchem.0c02457
Anal. Chem. 2020, 92, 12111−12115

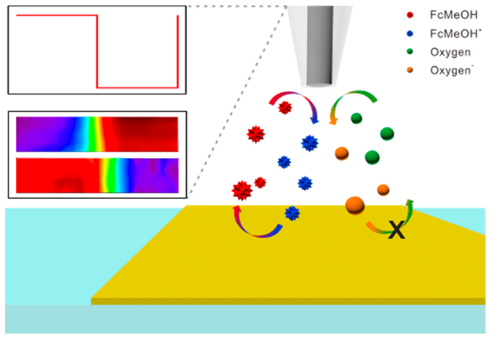

Figure 1. Schematic illustration of double-target-response P-SECM.

information for studying the life states of the cells. Furthermore, it would also determine the electrochemical behavior of different redox mediators on other targets and reveal the relevance among them.

The programming of P-SECM was based on HEKA SECM. For instance, a waveform for double-target-response P-SECM, taking ferrocenemethanol (FcMeOH) and oxygen as redox mediators, was set up (Figure 2A). Chiefly, the responsive

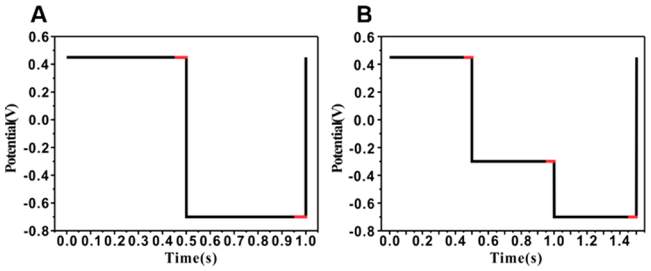

Figure 2. Potential−time waveform of double-target response P-SECM (A) and triple-target response P-SECM (B). Red parts indicated the time position where the current data was recorded.

signal current was obtained by biasing the tip potential into the target's oxidation or reduction steady-state potential, according to the waveform. This means that the signal current was obtained in the steady-state range of the target molecule. As for this double-target response, the potential changes from the steady-state potential of FcMeOH to that of oxygen. The switch of potential led to the appearance of charging current. In this case, the biased potential was held for 0.5 s to reduce the charging current by more than 95%,[14] and only the current data in the last 50 ms of 0.5 s was recorded and analyzed, hence, increasing the signal-to-noise ratio. The signal current value was the average of those data recorded in that 50 ms. Some other parameters related to signal acquisition were explained in detail in the Supporting Information.

For the waveform of more targeted response P-SECM, the difference is to add another potential pulse corresponding to the additional mediator into the waveform. Taking triple-target-response P-SECM as the example, the steady-state potentials of FcMeOH, hexaammineruthenium(III) ($Ru(NH_3)_6^{3+}$), and oxygen were assembled in one waveform (Figure 2B). Also the duration of each potential was 0.5 s, and only the current data in the last 50 ms of each 0.5 s was recorded.

The SECM imaging of a metal strip on a piece of glass was exhibited using both traditional SECM (T-SECM) and P-SECM. For this system, FcMeOH, $Ru(NH_3)_6^{3+}$ and oxygen were used as the redox mediators. It was well-known that in T-SECM, positive feedback occurred on the metal part when FcMeOH and $Ru(NH_3)_6^{3+}$ were the mediator. However, when it came to oxygen, a negative feedback phenomenon appeared, holding the tip above the metal part. This is because the reduction product of oxygen under −0.7 V of the tip potential would not be reoxidized to oxygen, thus the tip would not collect the oxygen generated from the substrate. The metal strip is on the glass, not inlaid, so that the plane of metal strip is a little higher than that of glass, leading to a shorter distance between the tip and metal strip, compared with that on the glass. In that case, the effect of negative feedback was stronger as the tip was scanning above the metal strip.

When three or more targets were in one system, there was a point on data processing that needed to be noticed. Taking FcMeOH, $Ru(NH_3)_6^{3+}$, and oxygen as the example, when the tip potential was −0.7 V, the reduction current consisted of the reduction of $Ru(NH_3)_6^{3+}$ and oxygen, since the diffusion reductive potential of $Ru(NH_3)_6^{3+}$ was −0.3 V, more positive than −0.7 V. The data of oxygen's reduction current ought to be the difference between the current under −0.7 V and −0.3 V. P-SECM images of the metal strip under −0.3 V and −0.7 V were exhibited in Figure 3A,B. The positive feedback under

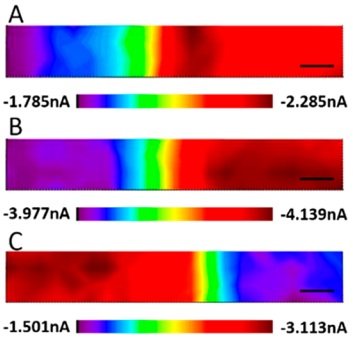

Figure 3. P-SECM imaging of the metal strip in 0.5 mM $Ru(NH_3)_6^{3+}$ with 0.1 M KCl at the same position. The tip was biased to −0.3 V (A) and −0.7 V (B). The data in (C) was the difference between the data in (A) and (B).

−0.3 V was obviously corresponding to the generation of $Ru(NH_3)_6^{3+}$ from the conductive substrate. However, the positive feedback phenomenon in Figure 3B demonstrated that the effect of $Ru(NH_3)_6^{3+}$'s positive feedback was stronger than the negative feedback effect of oxygen. The current data in Figure 3C was the difference between the data in Figure 3A,B, showing that the negative feedback phenomenon was totally attributed to the nongeneration of oxygen from the substrate.

As for the contrast on imaging by two methods, the same effects of positive and negative feedback were exhibited using T-SECM (Figure 4A) and P-SECM (Figure 4B). This phenomenon demonstrated that this P-SECM method could accurately and effectively distinguish the positive and negative feedback, demonstrating its feasibility on imaging. Figure 4 shows that when FcMeOH was as the mediator, the highest positive feedback normalized current obtained by P-SECM was 1.30 (Figure 4B-1), larger than that by T-SECM (1.09 in Figure 4A-1). Also the highest positive feedback normalized current in Figure 4B-2 (1.20) was larger than 1.08 in Figure 4A-2, using $Ru(NH_3)_6^{3+}$ as the mediator. Obviously, the normalized positive feedback current obtained by P-SECM was a little higher than that by T-SECM, because the charging

https://dx.doi.org/10.1021/acs.analchem.0c02457
Anal. Chem. 2020, 92, 12111−12115

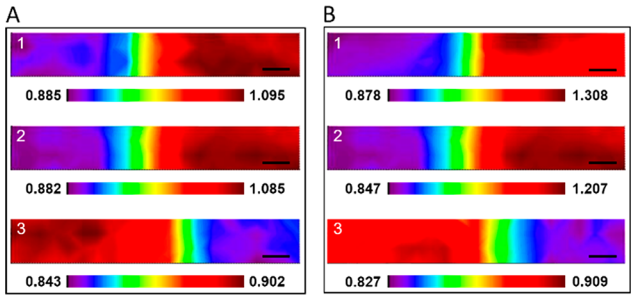

Figure 4. Imaging of a metal strip on glass using T-SECM (A) and P-SECM (B). A-1 and B-1 were imaged by FcMeOH. A-2 and B-2 were imaged by $Ru(NH_3)_6^{3+}$. A-3 and B-3 were by oxygen. The scale bar: 10 μm. The current bar was represented by the normalized current.

current, generated by the frequent potential switching, was not eliminated completely when the P-SECM was used.

SECM has been applied in cell imaging with many redox pairs as the mediators. Herein, FcMeOH, $Ru(NH_3)_6^{3+}$, and oxygen were used for cell imaging through both the T-SECM and P-SECM methods. FcMeOH and $Ru(NH_3)_6^{3+}$ exhibited negative feedback due to the smaller distance between the tip and cells.[15,16] As for oxygen, this negative feedback was contributed by not only the smaller distance but mainly cellular respiration, since oxygen went through cells by free diffusion and the cellular respiration of living cells consumed oxygen around the cell.[17]

Different from imaging by T-SECM, in which only one molecule responded during a single imaging, three images corresponding to three different molecules were obtained in one single imaging process when P-SECM was applied. This means that the cell status could be estimated by three molecules images obtained at the same time, instead of three different imaging periods with T-SECM. The cell images, using FcMeOH and oxygen as the mediators, obtained by T-SECM and P-SECM are shown in Figure 5A–D, respectively. Figure 5E,F exhibits the normalized current (I/I_0) of the lines crossing the cell in those images,[18,19] corresponding to FcMeOH and oxygen. The data by P-SECM (red curves in Figure 5E,F) were obtained in one single imaging. The black curve by T-SECM in Figure 5F was acquired about 20 min later than that in Figure 5E. The drop of I/I_0 from those curves represented the level of negative feedback affected by the tip–substrate distance (see the details in Supporting Information, Figure SI-3). This drop was not only influenced by the distance between the tip and cell but also by other factors like the permeability of the cell membrane. The membrane of a slightly active cell had less permselectivity, and most molecules could get through, hence increasing the diffusion of molecules and decreasing the negative feedback effect. Consequently, the degree of negative feedback in Figure 5E were approximate since the drop of I/I_0 was 0.165 and 0.183, respectively. However, in Figure 5F, the drop of I/I_0 was 0.185 when T-SECM was used, lower than 0.255 obtained by P-SECM. This decrease of negative feedback degree showed the change of mediator diffusion between the tip and cell at different times. Because oxygen was the mediator, the permeability was not the main factor while the respiration of the cell played a key role. This means the status of the cell, when the third image was in the scanning process, was different from that in the first image. Due to the simultaneous imaging of three molecules, the cell status in Figure 5E was the same as that in Figure 5F when P-

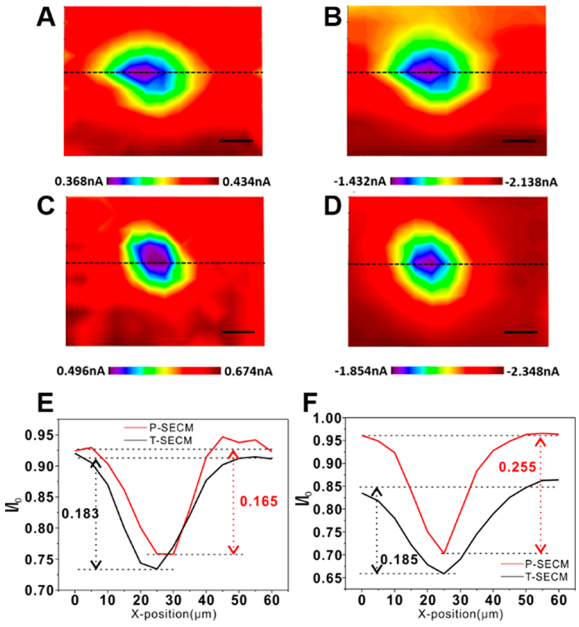

Figure 5. T-SECM (A and B) and P-SECM (C and D) imaging of a single cell, using FcMeOH (A and C) and oxygen (B and D) as mediators. The imaging environment was 0.5 mM FcMeOH in 20 mM HEPES (20 mM glucose) and 0.1 M KCl. (E) Data of the line crossing the imaging of the cell in (A) and (C). (F) Data of the line cross the imaging of the cell in (B) and (D).

SECM was used. This result demonstrated that imaging by P-SECM eliminated the error from different cell statuses caused by time consumption in a multiple imaging process when using T-SECM.

Different molecules respond differently to cells in different statuses. The membrane of a normal cell has good selective permeability while a dying cell's membrane has no such good selectivity. Even so, the SECM image scanned with a single mediator could not verify the cell status accurately since the negative feedback current was affected by not only the membrane permeability but also other factors, like cell height. Therefore, more information by different mediators was demanded to determine the cell status more accurately.

P-SECM was used to verify the cell status since this method could get more information at the same imaging period. Figure 6 shows the P-SECM images of a cell at two different statuses, normal or dying, using FcMeOH, $Ru(NH_3)_6^{3+}$, and oxygen as mediators. For FcMeOH, the images of normal and dying cell are exhibited in Figure 6A,D, and the data of a line crossing the cell in both images was extracted in Figure 6G. It could be observed that the negative feedback of the normal cell ($\Delta I/I_0 = -0.075$) was just a little more effective than that of the dying cell ($\Delta I/I_0 = -0.06$). This might be because the dying cell's membrane permeability increased so that a little extra FcMeOH crossed the cell membrane, which weakened the negative feedback effect. It has to be mentioned that FcMeOH can also partially cross the membrane of normal cells due to its hydrophobicity.[20] That was why the difference of negative feedback degree toward the normal and dying cell was not so obvious. Furthermore, this similar drop of I/I_0 showed that the distance between the tip and the normal cell was almost the same as that between the tip and the dying cell, indicating that the heights of the normal and dying cells were similar. Therefore, the error caused by the height difference was

https://dx.doi.org/10.1021/acs.analchem.0c02457
Anal. Chem. 2020, 92, 12111–12115

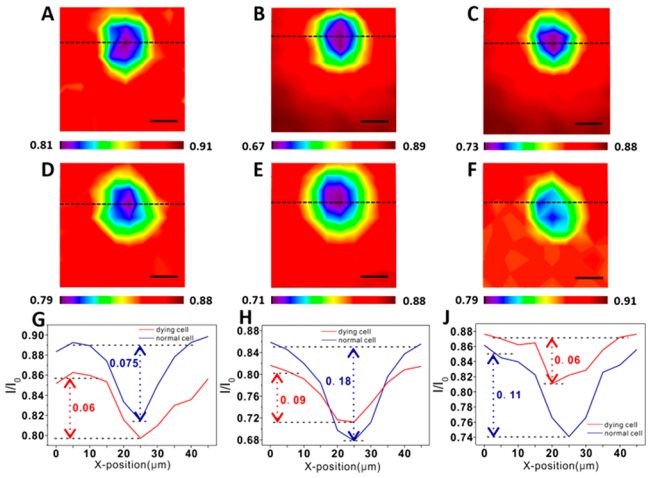

Figure 6. Imaging of normal (A, B and C) and dying (D, E and F) cells using P-SECM. FcMeOH (A, D), $Ru(NH_3)_6^{3+}$ (B, E), and oxygen (C, F) were used separately as mediators. The scale bar: 10 μm. Data of the line crossing the cell were exhibited in (G), (H) and (J). The red curve was represented for dying cells, and the blue curve was for normal cells.

eliminated. Results corresponding to $Ru(NH_3)_6^{3+}$, a hydrophilic mediator which might not cross the membrane of normal cells, are exhibited in Figure 6B,E,H. The negative feedback degree of the normal cell ($\Delta I/I_0 = -0.18$) was stronger than that of the dying cell ($\Delta I/I_0 = -0.09$) due to the change of membrane permeability.

As shown in Figure 6C,F,J, the drop of I/I_0 for the dying cell ($\Delta I/I_0 = -0.06$) was weaker than that for the normal cell ($\Delta I/I_0 = -0.11$) using oxygen as a mediator. This weakened degree of negative feedback was caused by not only the increased membrane permeability but also the vanishing respiration activity of the dying cell. The latter occupied the main position because oxygen could go through the cell by free diffusion. Note that this single comparison by oxygen, or FcMeOH, or $Ru(NH_3)_6^{3+}$ was not accurate and specific enough to demonstrate the unknown cell status. More information was needed to analyze and get a conclusion. According to the discussion above, the FcMeOH image eliminated the error from cell height and the $Ru(NH_3)_6^{3+}$ image verified the change of membrane permeability. Moreover, the oxygen image demonstrated the weaker respiration so that all three of these images determined the dying cell status accurately.

In conclusion, this work demonstrated that a multitarget-response P-SECM was feasible in feedback mode and the signal-to noise ratio was enhanced due to the designed waveform and data analysis. This new method was used in cell imaging through three different molecules at the same imaging period, eliminating the error caused by time consumption in multiple scans when T-SECM was used. Furthermore, an accurate verification of cell status was exhibited by analyzing the images of three different molecules using P-SECM. This method overcame the limitation of T-SECM, in which only one molecule was measured during the scanning process. Moreover, more electrochemical imaging information on targets would be investigated in one single imaging period so that the electrochemical behavior of different redox mediators on targets would be explored and the relevance among them would be studied.

■ ASSOCIATED CONTENT

Supporting Information

The Supporting Information is available free of charge at https://pubs.acs.org/doi/10.1021/acs.analchem.0c02457.

Experimental section, relative parameters of the protocol, and data analysis (PDF)

■ AUTHOR INFORMATION

Corresponding Authors

Fan Zhang − *School of Chemistry and Molecular Engineering, East China Normal University, Shanghai 200241, P. R. China*; orcid.org/0000-0003-4229-3916; Email: fzhang@chem.ecnu.edu.cn

Pin-Gang He − *School of Chemistry and Molecular Engineering, East China Normal University, Shanghai 200241, P. R. China*; Email: pghe@chem.ecnu.edu.cn

Authors

Xin Ning − *School of Chemistry and Molecular Engineering, East China Normal University, Shanghai 200241, P. R. China*

Tao Wu − *School of Chemistry and Molecular Engineering, East China Normal University, Shanghai 200241, P. R. China*

Qiang Xiong − *School of Chemistry and Molecular Engineering, East China Normal University, Shanghai 200241, P. R. China*

Complete contact information is available at: https://pubs.acs.org/10.1021/acs.analchem.0c02457

Notes

The authors declare no competing financial interest.

■ ACKNOWLEDGMENTS

This work was kindly supported by the National Nature Science Foundation of China (Grant No. 21575042).

■ REFERENCES

(1) Stender, A. S.; Marchuk, K.; Liu, C.; Sander, S.; Meyer, M. W.; Smith, E. A.; Neupane, B.; Wang, G.; Li, J.; Cheng, J. X.; Huang, B.; Fang, N. *Chem. Rev.* **2013**, *113*, 2469−2527.

(2) Dirks, R. W.; Molenaar, C.; Tanke, H. J. *Histochem. Cell Biol.* **2001**, *115*, 3−11.

(3) Lippincott-Schwartz, J.; Altan-Bonnet, N.; Patterson, G. H. *Nat. Cell Biol.* **2003**, *Suppl*, S7−S14.

(4) Watanabe, S.; Punge, A.; Hollopeter, G.; Willig, K. I.; Hobson, R. J.; Davis, M. W.; Hell, S. W.; Jorgensen, E. M. *Nat. Methods* **2011**, *8*, 80−84.

(5) Chen, H.; Puhl, H. L., 3rd; Ikeda, S. R. *J. Biomed. Opt.* **2007**, *12*, No. 054011.

(6) Lin, T. E.; Rapino, S.; Girault, H. H.; Lesch, A. *Chemical science* **2018**, *9*, 4546−4554.

(7) Bard, A. J.; Mirkin, M. V. *Scanning Electrochemical Microscopy*, 2nd ed.; CRC Press, 2012

(8) Polcari, D.; Dauphin-Ducharme, P.; Mauzeroll, J. *Chem. Rev.* **2016**, *116*, 13234−13278.

(9) Bard, A. J.; Li, X.; Zhan, W. *Biosens. Bioelectron.* **2006**, *22*, 461−472.

(10) Wessel, A. K.; Hmelo, L.; Parsek, M. R.; Whiteley, M. *Nat. Rev. Microbiol.* **2013**, *11*, 337−348.

(11) Paulose Nadappuram, B.; McKelvey, K.; Byers, J. C.; Guell, A. G.; Colburn, A. W.; Lazenby, R. A.; Unwin, P. R. *Anal. Chem.* **2015**, *87*, 3566−3573.

(12) Schrock, D. S.; Baur, J. E. *Anal. Chem.* **2007**, *79*, 7053−7061.

(13) Chen, X.; Botz, A. J. R.; Masa, J.; Schuhmann, W. *J. Solid State Electrochem.* **2016**, *20*, 1019−1027.

(14) Bard, A. J.; Faulkner, L. R. *Electeochemical Method: Fundamentals and Applications*, 2nd ed.; Wiley: New York, 2001
(15) Ueda, A.; Niwa, O.; Maruyama, K.; Shindo, Y.; Oka, K.; Suzuki, K. *Angew. Chem., Int. Ed.* **2007**, *46*, 8238−8241.
(16) Li, M. S. M.; Filice, F. P.; Henderson, J. D.; Ding, Z. *J. Phys. Chem. C* **2016**, *120* (11), 6094−6103.
(17) Takii, Y.; Takoh, K.; Nishizawa, M.; Matsue, T. *Electrochim. Acta* **2003**, *48*, 3381−3385.
(18) Koley, D.; Bard, A. J. *Proc. Natl. Acad. Sci. U. S. A.* **2010**, *107*, 16783−16787.
(19) Liu, B.; Rotenberg, S. A.; Mirkin, M. V. *Proc. Natl. Acad. Sci. U. S. A.* **2000**, *97*, 9855−9860.
(20) Henderson, J. D.; Filice, F. P.; Li, M. S. M.; Ding, Z. *ChemElectroChem* **2017**, *4*, 856−863.

https://dx.doi.org/10.1021/acs.analchem.0c02457
Anal. Chem. 2020, 92, 12111−12115